SCIREA Journal of Geosciences

http://www.scirea.org/journal/Geosciences

September 24, 2020

Volume 4, Issue 1, February 2020

Satellite - based Tropical Cyclone Track Assessment over Bay of Bengal using the GRIDSAT- B1 and SCATSAT- 1 retrievals and reanalysis data

Sutapa Chaudhuri[1,*], Jayanti Pal[1, 2], Ishita Sarkar[1], Indrani Ganguly[1, 3]

[1]Department of Atmospheric Sciences, University of Calcutta, Kolkata- 700 019, INDIA

[2]Department of Atmospheric Sciences, Central University of Rajasthan, Rajasthan - 305817, INDIA

[3] Department of Geological and Atmospheric Sciences, Iowa State University, Ames, Iowa 50011-3212, USA

Email: *sutapa.chaudhuri@gmail.com, jiban_samudra18@yahoo.com

ishitasarkar07@yahoo.com, iganguly@iastate.edu

Abstract

An attempt is made to perceive the dynamics for track evolution process of tropical cyclones over Bay of Bengal (BOB) by merging the satellite retrievals and reanalyses datasets. The systems investigated are the cyclonic storms KYANT, NADA and MAARUTHA belonging to the same category with different tracks. The cyclonic storm KYANT had looping track and had no landfall. However, NADA had westward track with landfall at southeast coast of India. The cyclonic storm MAARUTHA, on the other hand, had an eastward track with landfall over Myanmar. The analyses depict that the cloud clusters developed under different surface currents for the three systems. The result shows that the cloud clusters initially developed under surface westerly current for MAARUTHA. A tilt in vertical profile of vorticity is

observed with the track of KYANT and NADA while no such tilt is observed for MAARUTHA. The upper level divergence field is observed for NADA and MAARUTHA however, the divergence field in upper level was not discernible for KYANT. The result shows that the dynamics of the track evolution process for each system over the same ocean basin is rather different albeit the systems belong to the same category. Thus, the simulation of the track of cyclonic systems of the same category over a specific ocean basin with a single numerical model may not disseminate dependable information unless the surface current at the initial stage, vertical profile of vorticity and upper level divergence for each system are analysed and assimilated in the model correctly.

Keywords: Cyclonic Storm, track evolution process, Scatterometer, wind structure

Introduction

Forecasting with precision the track and the location of landfall of cyclonic storms (CSs) prevailing over any ocean basin is very important to cope with the associated disasters. Every year the north Indian Ocean (NIO) contributes about 5 to 6 tropical cyclones (TCs), approximately 7% of the world's total TCs (Mohanty and Gupta 2008). The damage from land falling TCs over the NIO has shown a steady increase due to growing population and structural imperfection. Most communities require a 12 to 24 h forecast to respond to a TC warning and at least a 12 h forecast before landfall for civil defence authorities to prepare for the storm hazards. The NOAA (National Oceanic and Atmospheric Administration) National Hurricane Centre has made a continual progress in improving forecasts of the TC track for the past 30 years over the Atlantic and east Pacific basins (Aberson 2001; Franklin et al. 2003). Likewise, over NIO, there has been significant progress and improvement in short range (1 to 3 days) track prediction in recent years (Mohapatra et al. 2013). In principle, the TCs move under the influence of its surrounding environment. Previous studies have suggested that TC track is primarily a function of the deep - layer wind field or steering flow (George and Gray 1976) and the advection of planetary vorticity by the TC circulation (Holland 1983). When the easterlies are added with the wind at certain level from the storm, the resulting effect forces the system to move in a westward direction (Emanuel 2003). The winds are not constant with height and thus, it complicates the movement. The wind shear around anti-cyclonic flow at the top of the TCs also impacts the movement and can influence the track of

the TCs. Current advancements in the use of sophisticated numerical methods, state of the art technologies, improved model resolution, physics, and data assimilation systems have shown some potential in track prediction over the NIO basin in recent years (Bhaskar Rao et al. 2009; Rappaport et al. 2009; Deshpande et al. 2010; Srinivasan et al. 2012; Osuri et al. 2012; Chaudhuri et al. 2014; and many others). In the year 2009, the India Meteorological Department (IMD) has extended the objective of TC track forecast validity period up to 72 hrs and subsequently up to 120 hrs in the year 2013 (Mohapatra et al. 2015). Mohapatra et al. (2013) found that the average direct position error (DPE) in TC track forecast over the NIO has decreased at the rate of about 7.3 km per year during 2003 – 2011 for 24 hrs forecasts. Osuri et al. (2013) observed that the high resolution meso-scale models resulted in substantial reduction in overall track forecast errors (8% to 24%) over NIO. Chaudhuri et al. (2014) implemented the multilayer feed forward neural network models for forecasting the track of tropical cyclones over the NIO. The neural net with 10 input layers, 2 hidden layers with 5 hidden nodes and 2 output layers provided the best forecast for the track of the TC over NIO. Though the TC track forecasts have been steadily improving for several decades, some uncertainty still remains due to variation in track forecast errors with respect to type of track, season of formation, intensity of the TC, etc. (Leroux et al. 2018). Track forecast errors over the NIO are still high relative to those over the Atlantic and Pacific Oceans (Mohapatra et al. 2013). The forecast uncertainty exists with position error to vary from less than 50 km to more than 500 km in a 3 - day forecast due to the chaotic nature of the atmosphere as well as the imperfection of NWP system (Ramarao et al. 2015). Accurate numerical prediction of TC track forecast is highly dependent on the quality of the initial state, resolving the in situ TC circulation, improving the understanding of rapid changes in TC track, and the accurate representation of physical and dynamical processes in the models (Mohanty et al. 2019).

The scatterometers on - board satellites are among such instruments that have capability of measuring both wind speed and wind direction over the ocean surface (Jaiswal et al. 2019). The present research aimed at identifying the dynamics of the track evolution process of the CSs over BOB using the GRIDSAT-B1, SCATSAT-1, NOAA and NCEP / NCAR retrievals and reanalyses datasets by analysing the variability in brightness temperature, daily sea surface temperature (SST) anomaly, ocean vector wind at 10 m, wind and its divergence at 200 hPa level, low - level convergence at 850 hPa level, vertical profile of vorticity from 1000 to 100 hPa levels along with vertical velocity. The three cyclonic systems considered in this study belong to the category of cyclonic storms, however, the routes of the track for each are

observed to be different when the surface and vertical structure are noticed. The cyclonic storm KYANT is found to have looping track feature; NADA has leftward track the cyclonic storm MAARUTHA has rightward track.

Data and Methodology

The gridded satellite (GRIDSAT-B1) data provides a uniform set of quality controlled geostationary satellite observations for the visible, infrared window and infrared water vapour channels. GRIDSAT-B1 uses the International Satellite Cloud Climatology Project (ISCCP) B1 dataset providing coverage every 3 hours from 1980 to the present, and is updated quarterly as possible. The data of brightness temperature has been used from GRIDSAT - B1 data (Knapp et al. 2011).

The daily sea surface temperature (SST) anomaly data has been collected from NOAA Optimum Interpolation SST V2 High Resolution Dataset (Reynolds et al. 2007). The NOAA 1/4° daily Optimum Interpolation SST or daily OISST is an analysis constructed by combining observations from different platforms (satellites, ships, buoys) on a regular global grid.

The daily wind components (zonal, meridional and vertical) at different pressure levels (1000 to 100 hPa) have been used from National Centres for Environmental Prediction – National Centre for Atmospheric Research (NCEP-NCAR) reanalysis (Kalnay et al. 1996). It provides 6 - hourly data, daily and monthly meteorological data since 1948 to present at 2.5° x 2.5° grid resolution. The local ingestion process took only the 0Z, 6Z, 12Z, and 18Z forecasted values, and thus only those are used to make the daily time series and monthly means in this study. The vertical vorticity and upper level (200 hPa) divergence has been computed from this data.

The Scatterometer Satellite-1 (SCATSAT-1) has been developed by ISRO Satellite Centre, Bangalore, India and its payload was advanced by Space Applications Centre (SAC), Ahmedabad, India for weather forecasting, cyclone prediction, and tracking services to India. The SCATSAT – 1 was launched on 26th September 2016. The daily surface wind data has been utilised from newly launched SCATSAT-1 dataset that provides ocean wind vector since October 2016 at 25 km spatial resolution. The surface convergence has been calculated from SCATSAT-1 data.

Results and Discussion

The present study selected three cyclonic systems, namely, KYANT, NADA and MAARUTHA of analogous category occurred over the ocean basin (BOB) to comprehend the dynamics of the track evolution process of each using GRIDSAT-B1, SCASAT-1, NOAA and NCEP / NCAR datasets.

CASE I: KYANT

The first cyclonic storm (CS) detected by SCASAT-1 is KYANT that occurred over BOB during 21st to 28th October, 2016. The deep depression developed over east - central BOB was observed to move west northwestward and subsequently intensified into a CS in the morning of 25th October over east - central BOB. The track of the cyclone KYANT was monitored and predicted continuously since its inception by the IMD. The SCATSAT - 1 level 3W products depict wind circulation at the mature stage of KYANT (Fig. 1a). The track of the cyclone over BOB during 21st to 28th October, 2016 is also observed by the IMD (Fig. 1b).

The cyclonic storm KYANT is considered first in this investigation to perceive the dynamics of the cloud cluster during its development process by analyzing the dataset of surface wind (in vector), SST anomaly (in shades) and brightness temperature (in contours) (Fig. 2). To identify cloud cluster, brightness temperature should be less than 230K for KYANT. The day – to - day development of KYANT from 19th October 2016 (two days prior to the initiation) to 28th October 2016 has been analysed. An anticlockwise wind circulation is observed near (13°N; 90°E) on 19th October (Fig. 2a). The wind in the lower part of the circulation is observed to be roughly westerly while the wind in the upper part is easterly. The red contours indicate the formation of cloud clusters, even though widely spread. The anticlockwise circulation is found to be almost at the same position on 20th October (Fig. 2b). The wind in the lower part of the circulation turned more to south-westerly direction. The cloud clusters became noticeably compact and found to be located near (3°N; 90°E). However, on 21st October, the anticlockwise circulation developed as a depression (D) over east central BOB (Fig. 2c). The winds in the lower part of the circulation are found to be southwesterly while the wind in the upper part is in easterly direction. Subsequently, a number of cloud clusters have been observed over the western side of the anticlockwise circulation near (13°N; 85°E). The anticlockwise circulation is observed to move east - northeastward towards the Myanmar coast on 22nd October (Fig. 2d). The winds in the lower part are found to move toward north-east direction while the winds at upper part show southwestward direction. The

wind on the left of the circulation is found to be slightly north – westerly direction while on the right, the wind is southwesterly. A well-defined cloud cluster is observed on the west-southwestern side of the circulation. The circulation is observed to intensify into a deep depression (DD) on 23rd October (Fig. 2e). The winds in the lower part of the circulation are found to be westerly while the wind in the upper side is observed to be in easterly and northeasterly direction. The wind flow is north-northwesterly on the left of the circulation while on the right it is observed to be southerly. A well-defined cloud cluster is located at west of the anticlockwise circulation, just on its periphery. The SST anomaly is observed to be negative at the center of the deep depression and positive in the surrounding region. The change in direction of the movement of the system is well captured by the surface wind plot and the system is observed to re-curve west-northwestwards on 24th October (Fig. 2f). The wind in the southern part of the circulation is almost westerly while in the left it is northwesterly and in the right it is southerly. The cloud cluster is found to be located around (15°N; 90°E). The system intensified into a CS over east-central BOB on 25th October (Fig. 2g). The position of the cloud cluster is found almost at the center of the circulation. The wind on the left of the CS is observed to be northerly and on the right, it is southerly. The center of the cyclone has both, positive and negative SST anomaly, whereas the SST anomaly is found to be positive in the surrounding regions. The cyclonic system is observed to change further its direction of movement and moved west-southwestwards on 26th October (Fig. 2h). The wind to the right of the cyclone is found to be southeasterly while to the left is northeasterly. Wind at the lower part of cyclonic circulation blows from west-northwest to east-northeast. The cloud cluster is found to be located on the eastern periphery of the cyclonic system. The SST anomaly in the southern part of the circulation is found to be negative while in the northern part it is observed to be positive. On 27th of October (Fig. 2i), the system is observed to move further westward, approaching close to the eastern coast of India. To the right of the circulation, the wind flow is observed to be west-northwesterly towards the landmass of India and the cloud cluster is found to be situated near (15°N; 89°E), over the eastern periphery of the depression. The system is observed to weaken over west-central BOB off the Andhra Pradesh coast by the morning of 28th October. The cloud cluster is observed to dissipate (Fig. 2j). The SST anomaly in the low pressure zone is found to be positive.

The low level convergence (red contour), upper level divergence at 200 hPa (green contour) along with the wind shear between 850 and 200 hPa pressure levels (shaded) are plotted using GrADS software during cyclonic system KYANT to reveal the features of convergence and

divergence associated with the cyclone. A small region with highest wind shear (deep blue) is found between 80°E and 90°E longitude and subsequently it decreased outward on 19th October stretching along the equatorial belt from 60°E to beyond 90°E longitudinally and from the equator to about 10°N latitude (Fig. 3a). The upper level divergence is also observed over the central and eastern BOB region, the values ranging from 0.9 to 0.3. It is superimposed over low level convergence with values ranging from -0.8 to -0.2. The region of high wind shear is observed to increase and reside over the equatorial belt, spreading more on 20th October (Fig. 3b). The upper level divergence, ranging from 0.6 to 0.3 has been observed to spread over the central BOB. The divergence ranging from 1.2 to 0.3 is also seen over the Arabian Sea and southern BOB. It is superimposed partly over low level convergence with values ranging from -0.4 to -0.2. The upper level divergence is observed to be quite prominent while the low level convergence is not so discernible. The highest wind shear is observed over (1°-3°N; 75°- 85°E) which decreases outwards, spreading along the equatorial oceanic region on 21st October (Fig. 3c). The upper level divergence is observed over southern and central BOB. The highest value (1.2) of divergence is seen near (8°N; 90°E) which is found to diffuse outwards to 0.3. It is superimposed over a low level convergence, spreading over the whole BOB with a value of -0.2. High wind shear zone is observed over south-eastern BOB and over a small region of northern BOB along the coast of West Bengal and Odisha on 22nd October (Fig. 3d). The upper level divergence is seen to be high over south-eastern BOB ranging from 0.9 to 0.3 and over the Andhra coast, where the value decreases outwards to 0.3, spreading over the Andhra region. An area of low level convergence is observed over the central and east-central BOB region, the value being -0.2. High wind shear has been observed over extreme east-central BOB which is in decreasing trend outwards on 23rd October (Fig. 3e). Another region with moderate wind shear is observed over the Odisha coast in the northern BOB region. Continuous upper level divergence is found over the northern and east central BOB with a low value of 0.3 and moderate upper level divergence is found in the south-eastern BOB region. Low level convergence is not observed. Moderate to low wind shear is seen to spread over the southern and south eastern BOB region and a small area is observed near the Odisha and West Bengal coastal region on 24th October (Fig. 3f). The upper level divergence with values ranging from 0.6 to 0.3 is observed over the north eastern coast of India, spreading over (15° - 25°N; 80°- 90°E). The low level convergence is not apparent over the BOB region. Wind shear is almost absent over BOB region, except with low values over parts of Andhra and Odisha coasts and moderate to low values over the Myanmar landmass. This indicates the intensification of cyclone KYANT on 25th October (Fig. 3g). The upper

level divergence with a value of 0.3 is observed partly over the north eastern BOB and partly over the Myanmar landmass. The low level convergence is found to be absent. High to moderate wind shear is seen over the Andhra coast, north central BOB and partly over the landmass of Myanmar on 26th October (Fig. 3h). The upper level divergence with a value of 0.3 is found to spread over the north-central BOB and Myanmar landmass. The low level convergence with a value of -0.2 is observed over southern BOB near (5° - 8°N; 82° - 92°E). Areas with moderate to low wind shear are seen to spread over the central landmass of India, extending over north-central BOB to the landmass of Myanmar on 27th October (Fig. 3i). The upper level divergence with values ranging from 0.9 to 0.3 is observed to spread over north-eastern India and Myanmar and extending up to southern BOB region. The lower level convergence is absent, except for a very small region near (15°N; 93°E). Moderate to low wind shear is present only over parts of Myanmar and absent over other parts of BOB. The upper level divergence is present over the north-eastern landmass which extends to a very small region of the northern BOB on 28th October (Fig. 3j). The low level convergence is found to be absent. It is noticed that the gradual weakening of wind shear with the intensification of cyclone KYANT is well captured in the wind shear plot. Prior to the development of KYANT as cyclonic storm the low level convergence zone has been observed to be present near the zone of upper level divergence. As the system is observed to intensify the convergence zone started weakening and the divergence zone is observed to strengthen.

The vertical profile of vorticity (contour) and vertical velocity (shades) during cyclone KYANT depict that the vertical velocity is positive and the highest value of 0.04 to 0.06 is confined between 650 and 800 hPa pressure levels on 19th October, 2016 within 80°E to 85°E longitude (Fig. 4a). The positive vertical velocity indicates updraft. However, beyond 85°E longitude the vertical velocity becomes negative indicating a downdraft. The core of maximum vertical vorticity is observed between 85.5°E and 92°E and up to 700 hPa pressure level. The value is found to decrease to 1 at 650 hPa level and subsequently to 0.5 at 450 hPa level between 85°E and beyond 100°E longitude. The vertical velocity is observed to be positive within 80°E to 85°E longitude between 350 hPa and 1000 hPa pressure levels on 20th October (Fig. 4b). The vertical velocity becomes negative for all pressure levels beyond 85°E longitude. The maximum vertical vorticity is centered near 90°E longitude between 900 and 800 hPa levels. The vertical vorticity is observed to decrease at 600 hPa and is observed to be 1 at 550 hPa level between 87°E and 95°E longitudes. The contours in this region have a slight northeasterly tilt. The lowest observed value of vertical velocity is 0.5 at 400 hPa level.

The vertical velocity is found to be positive within 80°E to 85°E longitudes and between 350 and 1000 hPa pressure levels. The vertical velocity is negative for all pressure levels indicating downdraft beyond 85°E longitude on 21st October (Fig. 4c) and is observed to be maximum up to 600 hPa pressure level between 88°E and 93°E longitudes. It decreases at 550 hPa between 86°E and 95°E longitudes which decreases further at 400 hPa pressure level. A north-northeastern tilt in vertical vorticity is observed up to 550 hPa level. The vertical velocity is found to be positive within 80°E to 84°E longitude between 500 and 1000 hPa pressure levels on 22nd October (Fig. 4d). However, the vertical velocity becomes negative for all pressure levels indicating a downdraft beyond 85°E longitude. No tilt in vertical vorticity is observed on 22nd October. The vertical velocity is found to be positive within 80°E to 87°E longitude between 400 and 1000 hPa pressure levels, which indicates upward motion on 23rd October (Fig. 4e). Nevertheless, the vertical velocity is negative for all pressure levels indicating downdraft beyond 87°E longitude. The vertical vorticity with a maximum core value of 1.5 is observed between 90°E and 96°E longitudes and up to 350 hPa pressure level. It is observed to decrease gradually with lowest core value of 0.5 at 250 hPa level between 88°E and 97°E longitudes. No tilt is observed in the vertical vorticity profile. The vertical velocity is found higher than previous days with maximum value > 0.1 within 80°E to 86°E longitude between 750 and 950 hPa pressure levels, indicating increased updraft capacity of the cyclonic system on 24th October (Fig. 4f). The vertical velocity is negative above 950 hPa pressure level indicating downdraft beyond 90°E longitude. The vertical vorticity, with a maximum core value of 2.5 is observed at 93°E longitude up to 380 hPa pressure level. It is noticed that the vertical vorticity profile gradually tilts north-westwards and attains a minimum value of 1 at 250 hPa level between 88°E and 97°E longitudes. Comparatively lower positive vertical wind velocity with maximum value ranging from 0.08 to 0.1 is located near 83°E longitude between 800 and 900 hPa pressure levels on 25th October (Fig. 4g). Another region of positive vertical velocity is observed, extending from 93°E to 98°E between 300 hPa and 700 hPa pressure levels. However, the vertical velocity is negative elsewhere. The vertical vorticity, with maximum core value 1.5, is observed between 88°E and 94°E and up to 380 hPa pressure level. It decreases outward with minimum value of 0.5 at 300 hPa pressure level and residing between 86°E and 96°E longitudes. Positive vertical velocity is found between 80°E and 90°E longitudes between 750 and 1000 hPa pressure levels on 26th October (Fig. 4h). Another region of positive vertical velocity is observed along 90°E to 95°E longitudes with a north-south stretch, one maxima lying between 150 and 300 hPa level and another between 400 and 500 hPa levels. The maximum vertical vorticity (2.5)

is found between 85° and 90°E longitudes up to 700 hPa pressure level. The value decreases outwards. The vertical vorticity profile with values from 1.5 to 0.5 is observed to spread beyond 95°E longitudes between 400 and 750 hPa pressure levels. A region of low vertical velocity, with values ranging from 0 to 0.02 is seen between 350 and 600 hPa levels, extending from 80°E to 87°E longitudes on 27th October (Fig. 4i). Another region with values 0 to 0.02 centered around 90°E longitudes extending from 200 to 380 hPa pressure levels is observed. All other areas exhibit negative vertical velocity indicating downdraft. The maximum core of vertical vorticity is observed between 84° and 86°E longitudes and between 650 and 1000 hPa pressure levels. It is observed to extend northeastward up to 95°E longitude between 500 and 800 hPa pressure levels. The lowest value (0.5) of vertical vorticity is seen between 400 and 1000 hPa levels with a longitudinal extent from 80°E to almost 100°E. A north - south stretch of positive vertical velocity centered at 90°E is seen on 28th October (Fig. 4j). Another region of vertical velocity, with values ranging from 0 - 0.04 is found near 80°E - 83°E between 550 and 200 hPa levels. Other regions exhibit negative vertical velocity indicating downdraft. Maximum core of vertical vorticity with the value of 1.5 is seen between 650 and 850 hPa pressure levels, with a longitudinal stretch from 82°E to 90°E. The lowest observed value is 0.5 extending from 80°E to 89°E between 500 and 1000 hPa. No tilt is seen in the vertical profile of vorticity.

CASE II: NADA

The Second cyclonic storm under investigation observed by SCASAT-1 is NADA with leftward track formed over southeast BOB in the evening of 29th November 2016. It moved initially northwestwards and intensified gradually into cyclonic storm over southeast BOB in the morning of 30th November 2016. The cyclone was monitored and predicted continuously since its inception by the IMD. The SCATSAT-1 level 3W products depict the wind circulation at mature stage of NADA (Fig. 5a). The observed track of the cyclone over BOB during 29th November 2016 to 2nd December, 2016 is presented in Fig. 5b.

The surface wind (in vector), SST anomaly (in shades) and brightness temperature (in contour) are plotted using GrADS software to analyze the surface dynamics for the development process of cloud clusters during cyclone NADA (Fig. 6). To identify cloud cluster, brightness temperature should be less than 230K for NADA. Day-to-day analysis has been carried out during the period from 27th November (2 days prior to the initiation of NADA) to 2nd December, 2016. The formation of an anticlockwise circulation is observed near (3°N; 90°E) on 27th November (Fig. 6a). The wind flow in the southern part of the circulation is observed

to be westerly while that in the northern part is northeasterly. The cloud clusters are visible throughout the region from 75°E to near 100°E longitudes and from the equator to 8°N latitudes. The system has been observed to move west - northwestward on 28th November (Fig. 6b). The winds in the right of the system are mostly westerly and south-westerly while those in the left are mostly northerly and north-easterly. The cloud clusters are present over the region as before. The system is observed near (6.5°N; 87.5°E) on 29th November (Fig. 6c). The winds in the southern part of the depression are mostly southwesterly and northwesterly while those in the northern part are easterly and north-northeasterly. The cloud clusters are observed over the northern periphery and south-eastern periphery of anticlockwise circulation. The system over southeast BOB is observed to move further west-northwestward and lay centered near (8°N ; 85°E) on 30th November (Fig. 6d). The wind flow in the northern part of the system is found easterly and northeasterly while in the southern part, the wind is westerly. The cloud clusters are concentrated mostly to the north of the anticlockwise circulation. The SST anomaly is found positive for most of the parts. The system is found to weaken and lay centered near (10.6°N; 81°E) over southwest BOB on 1st December (Fig. 6e). The wind flow is mostly southeasterly with traces of northeasterly flow. The cloud cluster is not found in the region. The system is observed to weaken further over southwest BOB off Tamil Nadu coast on 2nd December (Fig. 6f). The cloud cluster is dissipated as seen in the figure. The surface wind flow is found to be southeasterly and easterly. It is observed that the west-northwestward movement of the system is well captured by the surface wind plots. The cyclonic storm weakened over the sea under the influence of low SST over southwest BOB off Tamil Nadu coast.

The feature of convergence (red contour), upper level divergence at 200 hPa (in green contour) along with the wind shear (shades) between 850 and 200 hPa level associated with the cyclone NADA has been analyzed. The dynamics of the evaluation process depicts a low wind shear region over lower Andhra coast on 27th November (Fig. 7a). Another region of moderate to low wind shear is observed over south-eastern BOB near (5°N - 10°N; 90°E - 100°E). The upper level divergence is observed over central BOB extending from 70°E to 100°E longitude and from the equator to 15°N latitude with values ranging from 1.2 to 0.3 with outwards decreasing trend. This is superimposed by a region of low level convergence over extreme south-eastern BOB, spreading from 90°E to beyond 100°E longitude and from the equator to 10°N latitude. A moderate to low wind shear region is found over south-eastern BOB on 28th November (Fig. 7b). The upper level divergence, with values ranging from 1.2 to

0.3 is observed over south to south-central BOB. The low level convergence is not discernible. A moderately high to low wind shear region is seen over south-eastern BOB located near (5°-12°N; 90°-100°E) on 29th November (Fig. 7c). The upper level divergence with values ranging from 1.2 to 0.3 is observed over southern BOB, spreading from 80°E to 100°E longitude and 0° - 25°N latitude. The low level convergence was found to be absent. Moderately high to low wind shear is observed over central BOB which is found to stretch eastwards to the landmass of southern Myanmar on 30th November (Fig. 7d). The upper level divergence, with values ranging from 1.2 to 0.3, is noticed over the entire southern BOB, with higher values over south-western BOB. This is superimposed over a region of low level convergence near (8°N-15°N; 88°E-94°E). A narrow band of very low wind shear is observed to stretch from west to east, along central BOB on 1st December (Fig. 7e). High upper level divergence, with values ranging from 0.9 to 0.3 is seen over the landmass of India. The upper level divergence, with a low value of 0.3 is also found over central and north-central BOB. This is superimposed partly over a region of low level convergence near (12°-17°N; 90°-95°E). The wind shear over the BOB region is found to be absent on 2nd December (Fig. 7f). An upper level divergence is found over the landmass of central India to east central BOB, with values ranging from 0.6 (mostly over north-eastern and north-central BOB) to 0.3. Another area of upper level divergence is found over south-eastern and southern BOB. This is superimposed over a region of low level convergence extending from 90°E to beyond 100°E and from the equator to 10°N. The strengthening of upper level divergence with the intensification of cyclone NADA is evident from the above plot. The upper level divergence is also observed to shift westward.

The vertical profile of vorticity (contour) and vertical velocity (shades) during cyclone NADA depicts negative vertical velocity between 80°E and 100°E longitudes through all the pressure levels indicating strong downdraft on 27th November (Fig. 8a). The maximum core of vertical vorticity is seen between 600 and 700 hPa centered at 85°E and another region is seen over 93°E longitude, between 450 and 550 hPa pressure levels. The lowest observed value is 0.5 between 350 and 850 hPa pressure levels with a longitudinal extent of 80° to 95°E. The vertical velocity is found to be negative from 80°E to 100°E longitudes through all the pressure levels, indicating strong downdraft on 28th November (Fig. 8b). The maximum core value of positive vertical vorticity is found between 600 and 700 hPa pressure levels. The value decreases to 0.5 at 400 hPa level, extending from 80°E to 95°E longitudes. The vertical velocity is found to be negative between 80°E and 100°E longitudes for all pressure levels,

indicating downdraft on 29th November (Fig. 8c). The maximum core of positive vertical vorticity is centered along 90°E longitude, between 500 and 700 hPa pressure levels and also between 800 and 1000 hPa pressure levels. The value decreases gradually, with a minimum value of 0.5 at 300 hPa between 83° and 94°E longitudes. A slight north-western tilt in vertical vorticity is observed here. The vertical velocity between 80° and 100°E longitudes is found to be negative for all pressure levels, indicating downdraft, except for a small region along 95°E, between 100 and 250 hPa pressure levels on 30th November (Fig. 8d). The maximum core of positive vertical vorticity, with value 4, is located near 85° - 87°E longitudes between 800 and 950 hPa levels. It decreases gradually with lowest core value observed to extend up to 250 hPa. The contours in this region have a slight north-western tilt. Positive vertical velocity is observed in three different regions, first is observed over 90°E (value ranging from 0 - 0.01) between 800 and 950 hPa pressure levels; second is seen over 80°E longitude (values ranging from 0 - 0.06) between 250 and 510 hPa pressure levels; third positive vertical velocity is seen to be centered near 92°E (values ranging from 0 - 0.06) between 100 and 350 hPa pressure levels on 1st December (Fig. 8e). The vertical vorticity with a maximum core value of 4 is observed from 800 to 420 hPa pressure levels. Positive vertical velocity is seen along 85°E longitude between 800 and 1000 hPa pressure levels, and also at 200 hPa pressure level, indicating updraft. Another area of low positive vertical velocity is found to spread between 100 and 600 hPa pressure levels on 2nd December (Fig. 8f). A region of positive vorticity is found over 80° - 85°E, extending up to 400 hPa pressure levels. No tilt is observed.

CASE III: MAARUTHA

Cyclonic storm MAARUTHA, with rightward track, formed over southeast BOB in the morning of 15th April 2017. Moving northeastwards, it intensified into a deep depression (DD) over east-central BOB in the afternoon of 15th April and into a CS over east central BOB in the midnight of 15th April. The system crossed Myanmar coast near Sandoway (Thandwe) in the midnight of 16th April. SCATSAT-1 surface wind (Fig. 9a) indicates that the winds are observed around the system with maxima in northeast and southeast sector. It also agrees with best track estimates of the cyclonic storm MAARUTHA. Observed track of MAARUTHA over BOB during 15th April to 17th April, 2017 has been depicted in Fig. 9b.

The surface wind (in vector), SST anomaly (in shades) and brightness temperature (in contour) are plotted with GrADS software to identify the development process of cloud cluster during the cyclone MAARUTHA (Fig. 10). To identify cloud cluster, brightness temperature should

be less than 230K for MAARUTHA. Day-to-day analysis is carried out from 12th April 2017 (3 days prior to the initiation of MAARUTHA) to17th April, 2017. The wind flow patterns in south-eastern BOB is observed to form an anticlockwise circulation with center at (8°N; 90°E) on 12th April (Fig. 10a). The cloud clusters can be seen extending from 70°E to beyond 90°E longitude and from the equator to 18°N latitude. The winds in the lower and right part of the circulation are mostly westerly and south-westerly while in the upper and left part of the circulation winds are northerly. The SST anomaly near the center of the anticlockwise rotation is found to be positive. It is observed that the anticlockwise circulation shifted westwards with center at (8°N; 85°E) on 13th April (Fig. 10b). The wind in the southern side of the circulation is observed to be south-westerly and the winds from the east are observed to converge at the northern part of the circulation. The cloud cluster has shifted towards the east and north-east. More well-defined cyclonic circulation, compared to the previous day, is observed to form on 14th April (Fig. 10c). The cloud clusters are located mainly on the eastern and southern side of the circulation. The winds in the lower part of the circulation are found to be southwesterly while the wind in the right side is southeasterly. In the upper part, the wind flow is mostly easterly and to the left, it is northerly. The SST anomaly in the region is slightly positive in most of the parts. The system is observed to move north-eastward and lay centered near (15.3ºN; 91.0ºE) on 15th April (Fig. 10d). The cloud clusters are mostly concentrated over the eastern and southern side of the cyclone. The SST anomaly just beyond the eastern periphery of circulation is found to be positive. The CS is observed to move further northeastwards and attain its peak intensity in the early hours of 16th (Fig. 10e). The wind flow in the southern part of the system is westerly, while in the northern part, it is erratically easterly. On the eastern side of circulation, the wind flow is southerly. The SST anomaly at the center of the system is negative while on the southeastern side, it is highly positive. The cloud clusters are observed to move far away towards southeast direction. Moving nearly northeastwards, the system is observed to cross Myanmar coast near Thandwe and weakened thereafter on 17th April (Fig. 10f). The wind along the Myanmar coast is found mostly southeasterly with negative SST anomaly. The cloud cluster is found to be consistent. It is noticed that the system moves very fast under the influence of mid-latitude trough in the westerlies lying over India in the middle and upper tropospheric levels. The movement of MAARUTHA toward northeast direction throughout its life period is well captured by the surface wind plot and this movement may be under the influence of anti-cyclonic circulation located at the southeast of the system center.

The low level convergence (red contour), upper level divergence at 200 hPa (green contour) along with the wind shear between 850 and 200 hPa (shades) are plotted with GrADS software to understand the feature of convergence and divergence associated with the cyclone MAARUTHA. Moderately high to low wind shear is seen along the equatorial oceanic region, extending up to 10°N latitude at southern part of Indian landmass on 12th April (Fig. 11a). It extends up to about 5°N latitude over southern and south-east BOB. Upper level divergence over central and south-eastern BOB is seen, with high value (1.2) observed over south-eastern BOB and lower values (0.6 to 0.3) over central BOB. Another area of upper level divergence is noticed over north-eastern India, with highest value (0.9) in the center and decreasing gradually outwards. Lower level convergence, with values from -0.6 to - 0.2 is seen in the southern and south-eastern parts of BOB. A high wind shear zone is seen along equatorial oceanic region (0° - 6°N; 85° - 100°E) on 13th April (Fig. 11b). Another region of moderately high wind shear is seen over (0° - 5°N; 65° to 80°E). A region of low wind shear is observed near the Tamil Nadu coast. Upper level divergence, with the value of 0.3 is observed over most parts of BOB except western and west-central regions. Higher values of upper level divergence (ranging from 0.6 to 1.2) are observed over southern and south-central BOB and over the north-east Indian and Myanmar landmass. Over the entire southern BOB, the upper level divergence is superimposed over a low level convergence. Moderate to low wind shear is seen over southern BOB region, extending from 65° to 95°E and 0° to 10°N on 14th April (Fig. 11c). Continuous upper level divergence is found over the north-eastern landmass to entire BOB, with values ranging from 1.2 to 0.3. A region of low level convergence exists over southern and south-central BOB, with values ranging from -0.2 to -0.8. A high wind shear zone is found near 80°E and it gradually diffuses outwards, spreading over southern and south-eastern BOB. The upper level divergence with values from 1.2 to 0.3 exists over the entire BOB on 15th April (Fig. 11d). The lower level convergence is absent, except for a very small region around (2°N; 90°E) on 16th April (Fig. 11e). Moderately high to low wind shear is seen partly over the south-eastern part of BOB and partly over the landmass of Myanmar only. The upper level divergence with values 1.2 to 0.3 is observed over the north-eastern landmass of the Indian subcontinent and it extends along eastern BOB to southern BOB. A region of low level convergence (with value -0.2) is seen over south-eastern BOB, extending from 87°E - 98°E and 5°N - 15°N. Wind shear over BOB was practically absent. Eastern and southern parts of BOB had an upper level divergence, values ranging from 0.9 to 0.3 on 17th April (Fig. 11f). A small region of low level convergence is seen directly south of the landmass of India. Before MAARUTHA developed as cyclonic storm, low level convergence

zone is observed to present near the zone of upper level divergence. As system intensifies, convergence zone weaken and divergence zone is observed to strengthen.

Vertical profile of vorticity (contour) and vertical velocity (shaded) during cyclone MAARUTHA depicts that on 12th April, 2017 the vertical velocity is positive along 85°E longitude and for all pressure levels between 100 hPa and 1000 hPa (Fig. 12a). It decreases outward. Another region of high to moderate positive vertical velocity is observed at upper levels from 600 hPa to 100 hPa and centered along 97°E longitude. All other areas exhibit negative vertical velocity indicating downdraft. The maximum core of vertical vorticity, with value 1, is seen between 95°E and 97°E longitude and between 850 hPa and 950 hPa pressure levels. The value decreases to 0.5 between 750 hPa and 1000 hPa levels, lying across 95°E to 100°E longitudes. A north-west tilt in vertical vorticity profile has been observed. A region of maximum vertical velocity is seen over 85°E longitude, with the highest values between 800 hPa and 900 hPa pressure levels on 13th April (Fig. 12b). The vertical velocity values are observed to decrease outward. Another region with positive vertical velocity is seen from 90°E to 95°E. The positive values indicate regions of updraft. All other areas show negative vertical velocity, indicating regions of downdraft. The vertical vorticity contour is found to remain same as previous day. A north-south stretch of high to moderate positive vertical velocity centered at 84°E longitude is seen. The values of vertical velocity are found to be negative across all pressure levels, indicating downdraft beyond 90°E on 14th April (Fig. 12c). Two maximum core of vertical vorticity (value 1) are observed between 80°E and 88°E longitude; one is seen across 380 hPa to 450 hPa and other is found from 550 hPa to 650 hPa pressure levels. Within 80°E - 87°E longitude and between pressure levels 100 hPa and 950 hPa the vertical velocity is found to be positive indicating upward motion on 15th April (Fig. 12d). The vertical vorticity with maximum value 0.5 is seen along 90°E longitude at two different pressure levels; one between 400 hPa and 500 hPa and other between 850 hPa and 950 hPa. The vertical vorticity decreases gradually over a longitudinal extent of 87°E to 93°E, the magnitude decreasing to 0.5 at 300 hPa pressure level. It is observed that the region of positive vertical velocity has been extended from 80°E to beyond 90°E for all pressure levels except lower levels, where the positive vertical velocity is observed to extend up to 100°E on 16th April (Fig. 12e). The vertical velocity values are found negative from 92°E to 100°E and above 900 hPa pressure level, indicating regions of downdraft. The vertical vorticity with maximum value 2.5 is seen along 92°E, between 900hPa and 580hPa pressure levels. This value decreases gradually, becomes minimum (0.5) at 350hPa pressure level. No tilt is

observed. Positive vertical velocity is found between 80°E to 97°E and for all the pressure levels between 1000 hPa and 100 hPa on 17th April (Fig. 12f). The vertical vorticity maximum (value 2) is found to be centered near 92°E - 95°E and between 600 hPa and 750 hPa pressure levels. The minimum value is 0.5. The vertical vorticity profile has a north-western tilt across the longitudes and across 500hPa to 1000hPa pressure levels.

Summary

Identification of the dynamics for the track evolution process of three cyclonic systems of the same category prevailed over BOB is the main intend of this investigation.

The three cyclonic systems considered in this investigation are the cyclonic storms KYANT (21 – 28 Oct, 2016) with looping track, NADA (29 Nov – 02 Dec, 2016) with westward track and MAARUTHA (15 – 17 Apr, 2017) with eastward track.

The cyclone KYANT had a unique track feature that developed over BOB and moved east-north-eastward and again looped westward and dissipated over the ocean. The KYANT thus, did not have any land fall.

The cyclone NADA developed over BOB with westward track and had landfall at southeast coast of India.

The cyclone MAARUTHA had an eastward track and made the landfall over Myanmar.

The analytics show that the cloud clusters developed under different surface current for the three systems under investigation.

The cloud clusters are observed to develop in surface easterly current which is southern counterpart of cyclonic system in case of cyclone KYANT.

However, the cloud clusters have been developed by north - easterly current which is mainly northern counterpart of the cyclonic system in case of cyclone NADA.

The cloud clusters initially developed under surface westerly current in case of cyclone MAARUTHA. However, the cloud clusters have been observed to develop under south-westerly current which is south-east counter part of cyclonic system a day before MAARUTHA developed.

The wind shear for all the three cyclonic systems is found to be weak during the developing process, which is expected for the favourable development of the cyclonic storms.

The tilt (initially eastward and then looping characteristics at upper level and further westward) in vertical profile of vorticity has been observed with the track of cyclone KYANT and NADA (westward shift).

However, the upper level divergence field has been found to relate with NADA and MAARUTHA.

The study shows that the evolution process of track for each system is different though they belong to same category.

Surface current at initial stage, vertical profile of vorticity and upper level divergence might be able to give an insight on the dynamics of the evolution process of track for each system. However, the significance of these three features might depend on other factors required for the development of cyclones.

Acknowledgment

The corresponding author acknowledges the Space Application Centre, ISRO, India for providing the opportunity to participate in the SCATSAT 1 Application programme.

Figures

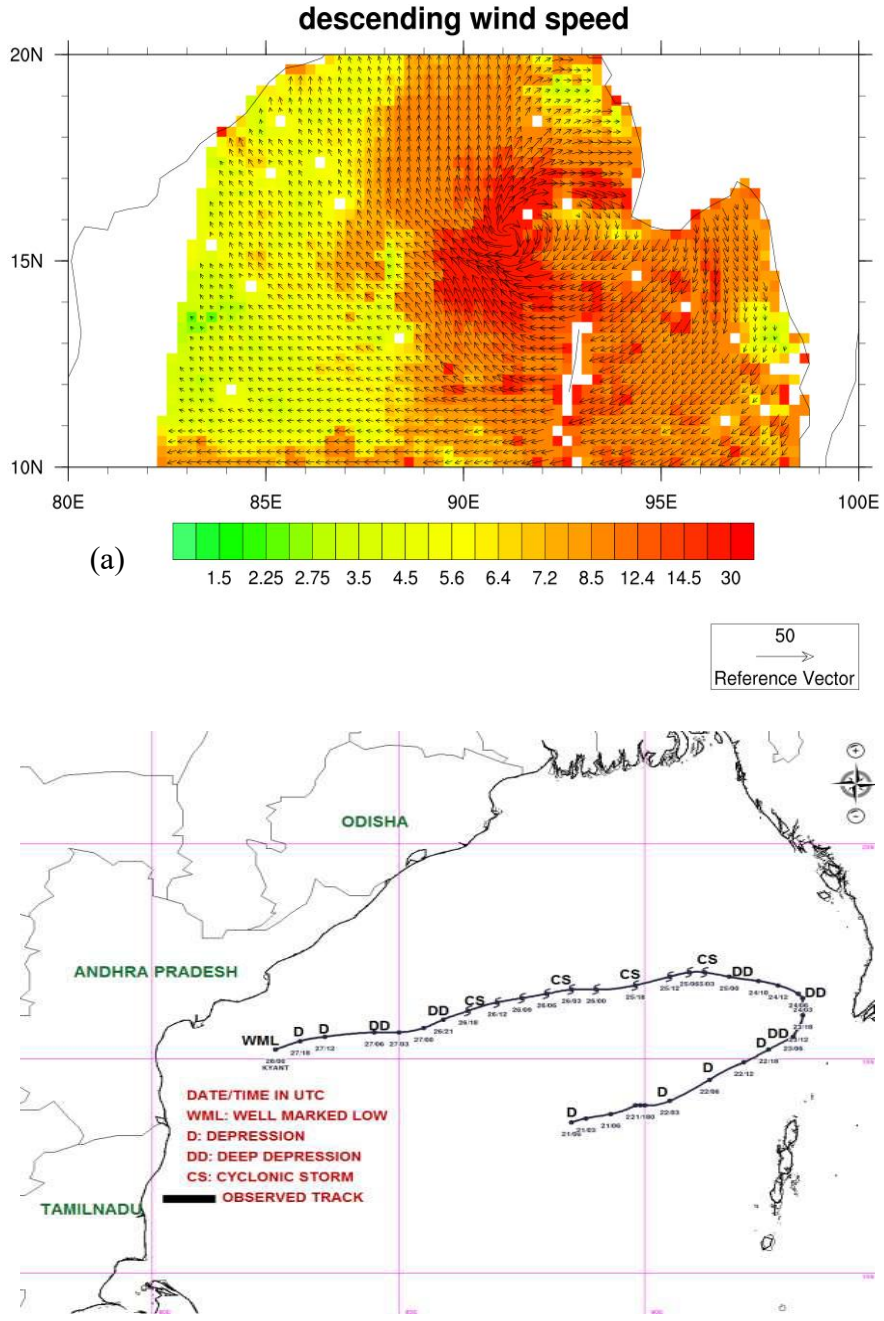

(a)

(b)

Fig. 1 The cyclone KYANT (a) at its mature stage as observed from SCATSAT-1 and (b) the track as observed by IMD

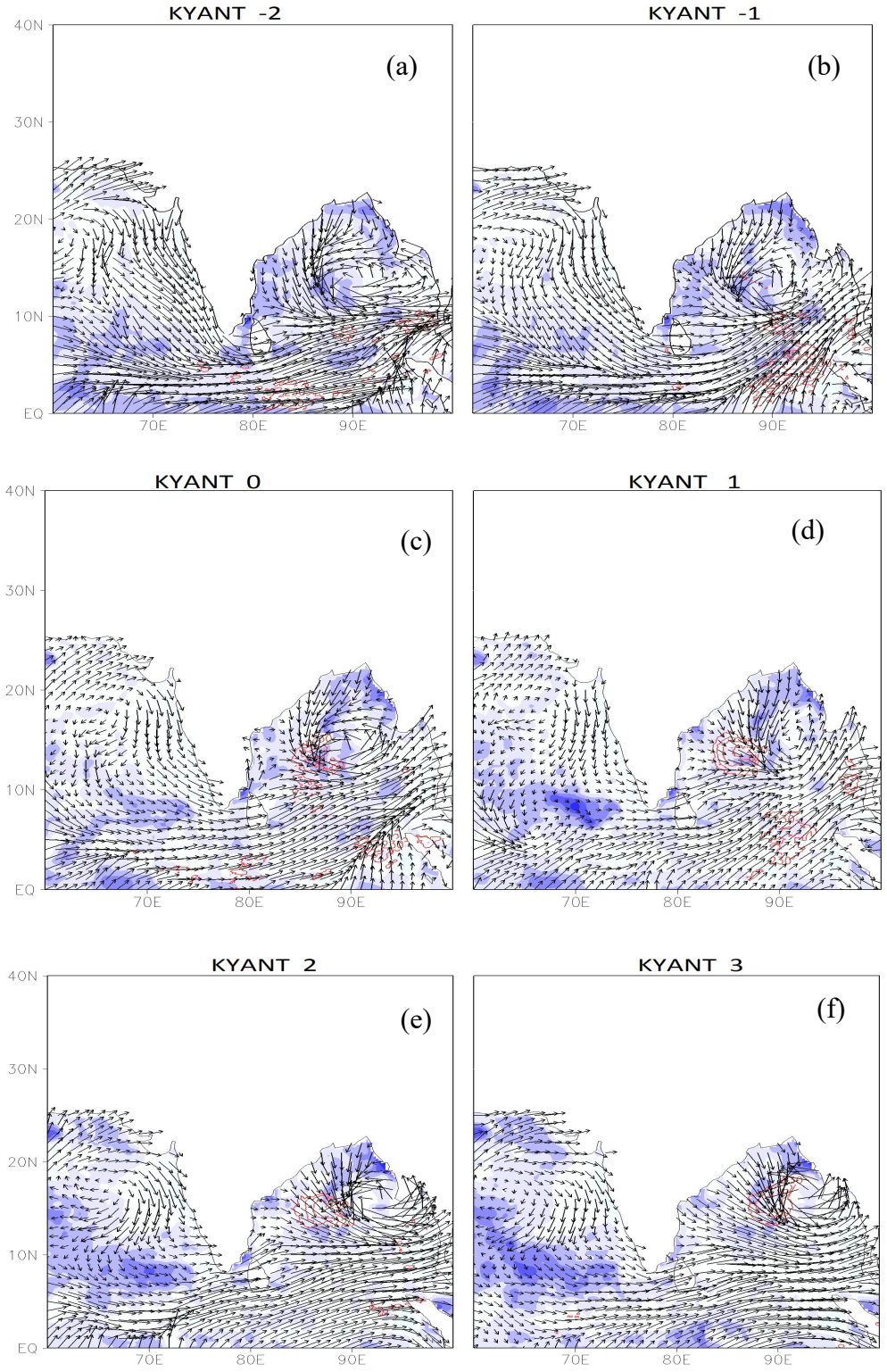

Fig. 2 Analysis of SST anomaly (shaded) and ocean vector wind at 10m (vector) along with position of cloud cluster as obtained from brightness temperature (red contour) for (a) 2 days before (b) 1 day before KYANT along with (c) day 1 (d) day 2 (e) day 3 and (f) day 4 of KYANT

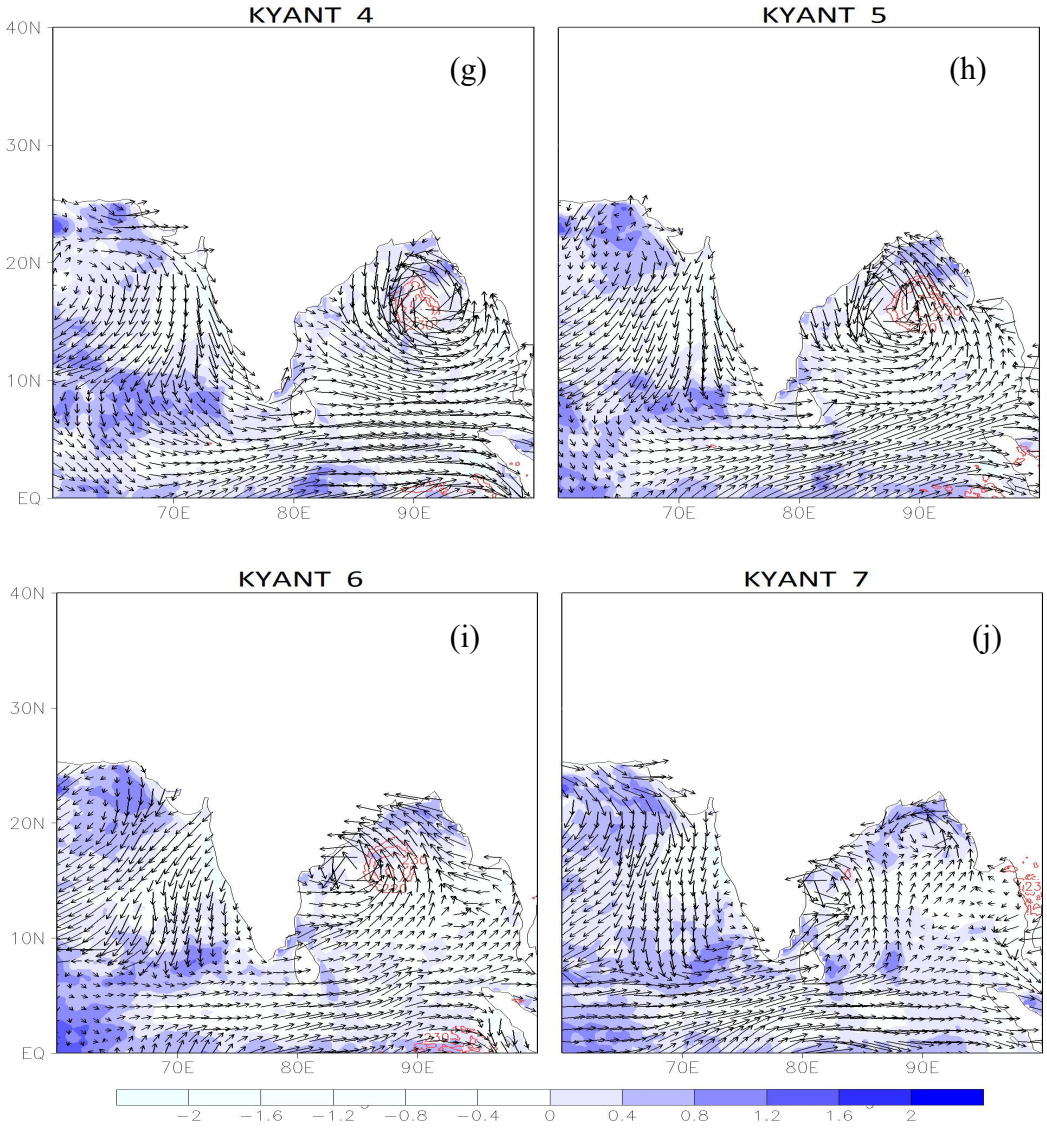

Fig. 2 (cont) Analysis of SST anomaly (shaded) and ocean vector wind at 10m (vector) along with position of cloud cluster as obtained from brightness temperature (red contour) for (g) day 5 (h) day 6 (i) day 7 (j) day 8 of KYANT

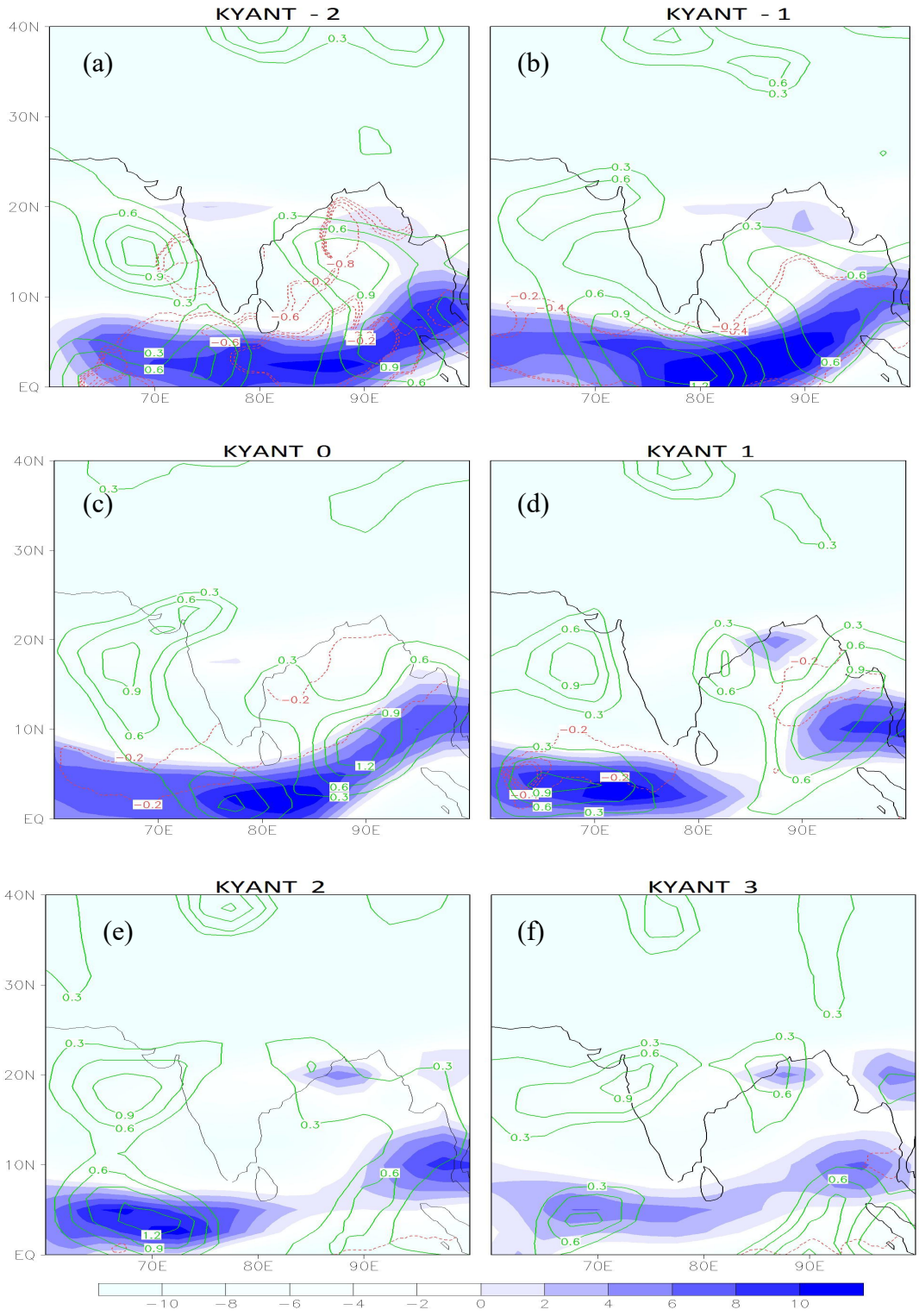

Fig. 3 Diagram shows wind shear between 850 hPa and 200 hPa (shaded), low level convergence (negative red contour) and upper level (200 hPa) divergence (positive green contour) for (a) 2 days before (b) 1 day before KYANT along with (c) day 1 (d) day 2 (e) day 3 and (f) day 4 of KYANT

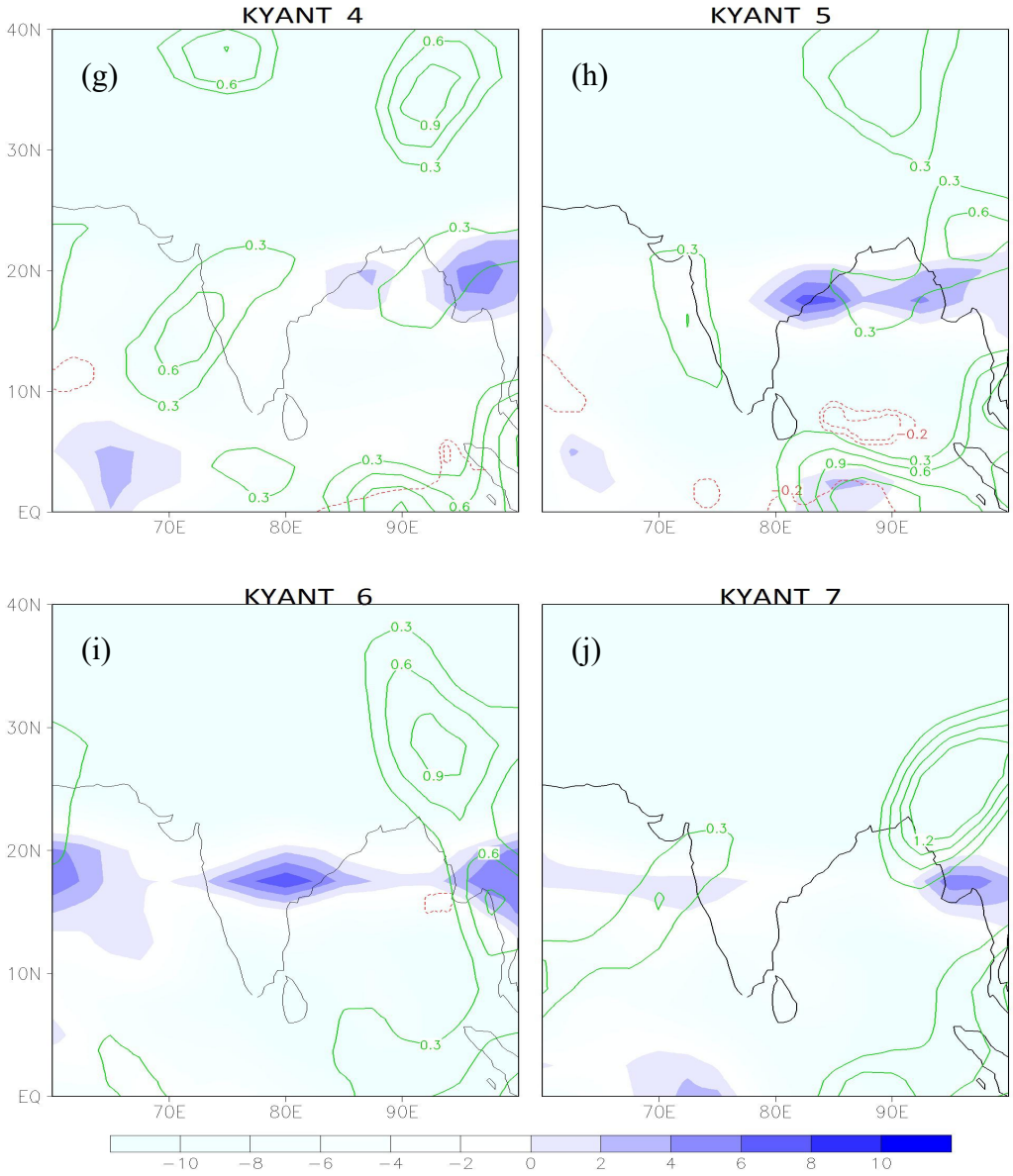

Fig. 3 (cont) Diagram shows wind shear between 850 hPa and 200 hPa (shaded), low level convergence (negative red contour) and upper level (200 hPa) divergence (positive green contour) (g) day 5 (h) day 6 (i) day 7 and (j) day 8 of KYANT

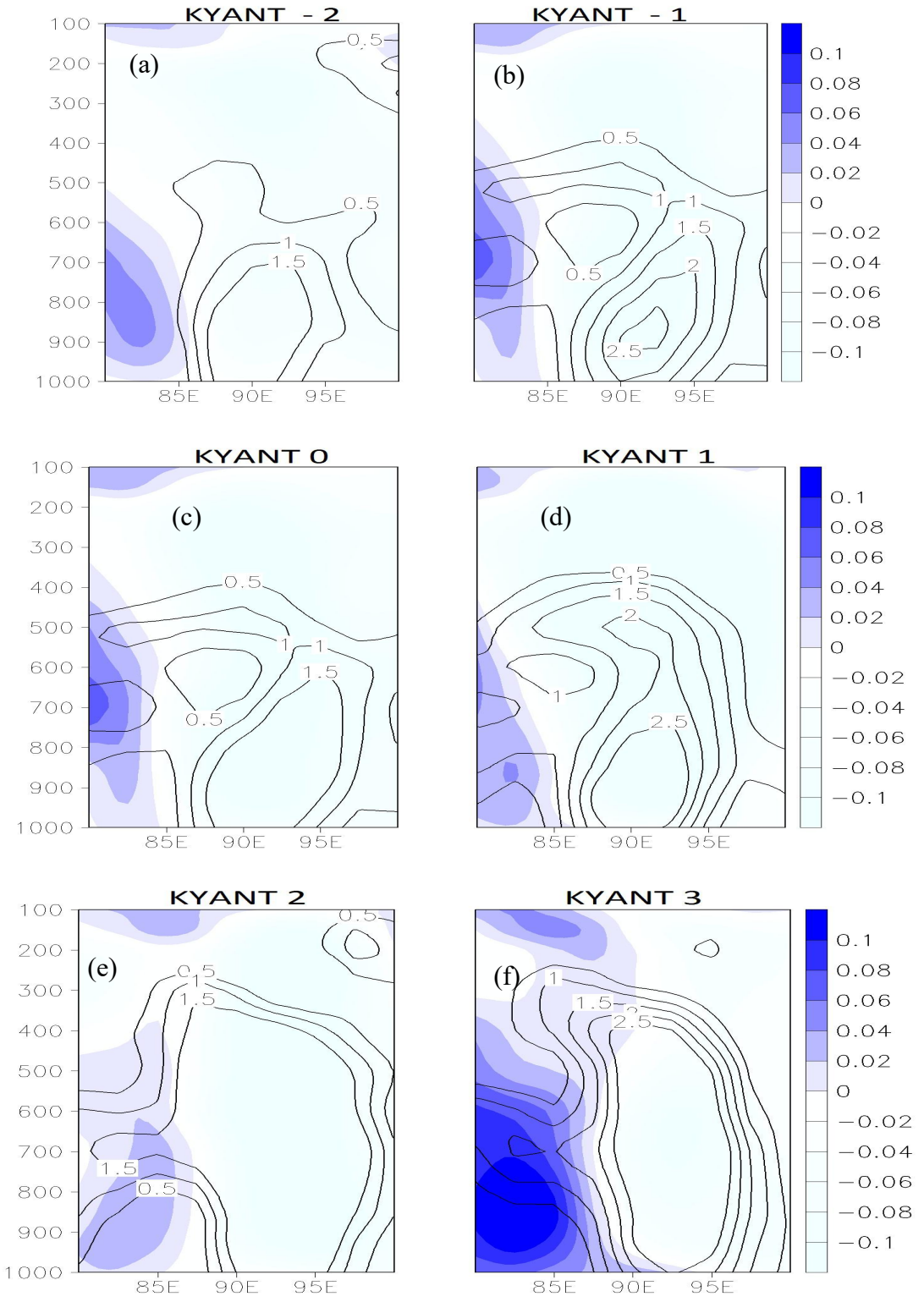

Fig. 4 Diagram shows vertical profile of positive vorticity (contour) and vertical velocity (shaded) for (a) 2 days before (b) 1 day before KYANT along with (c) day 1 (d) day 2 (e) day 3 and (f) day 4 of KYANT

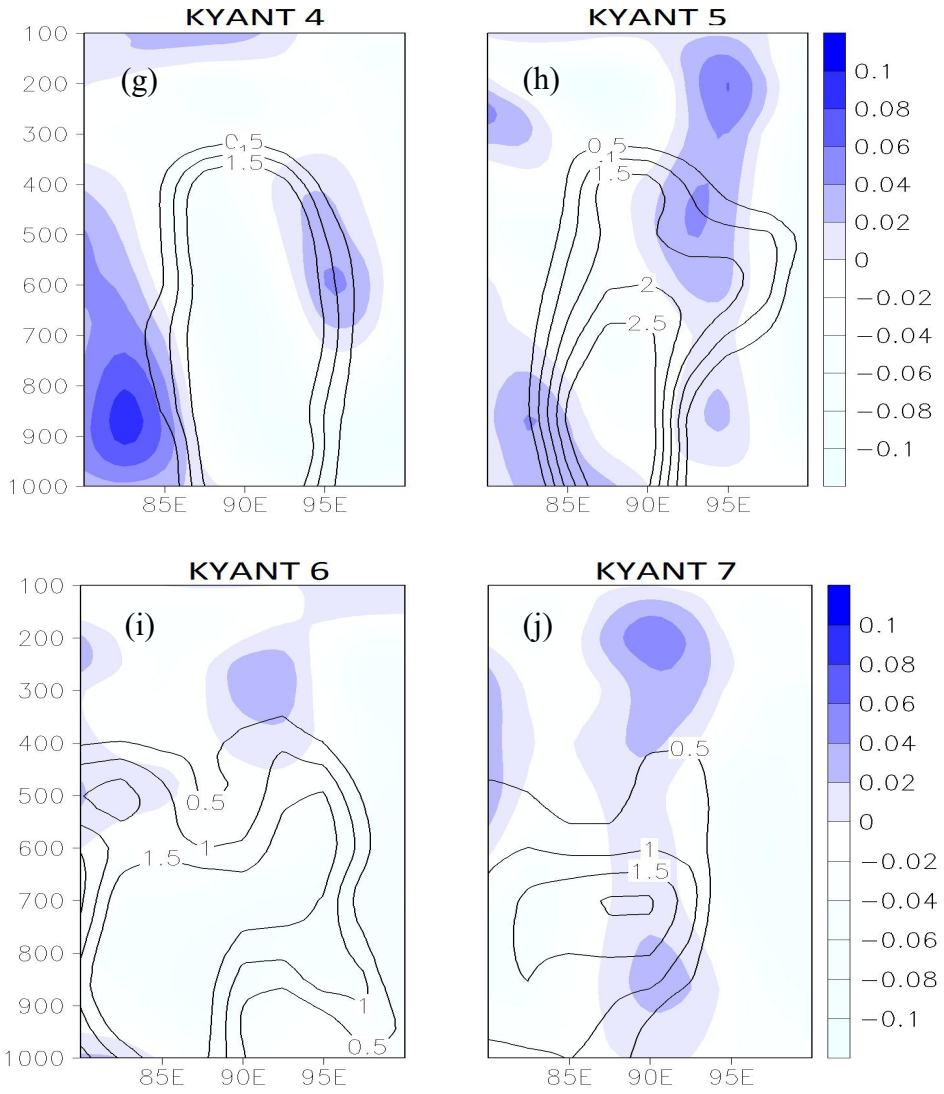

Fig. 4 (cont.) Diagram shows vertical profile of positive vorticity (contour) and vertical velocity (shaded) for (g) day 5 (h) day 6 (i) day 7 and (j) day 8 of KYANT

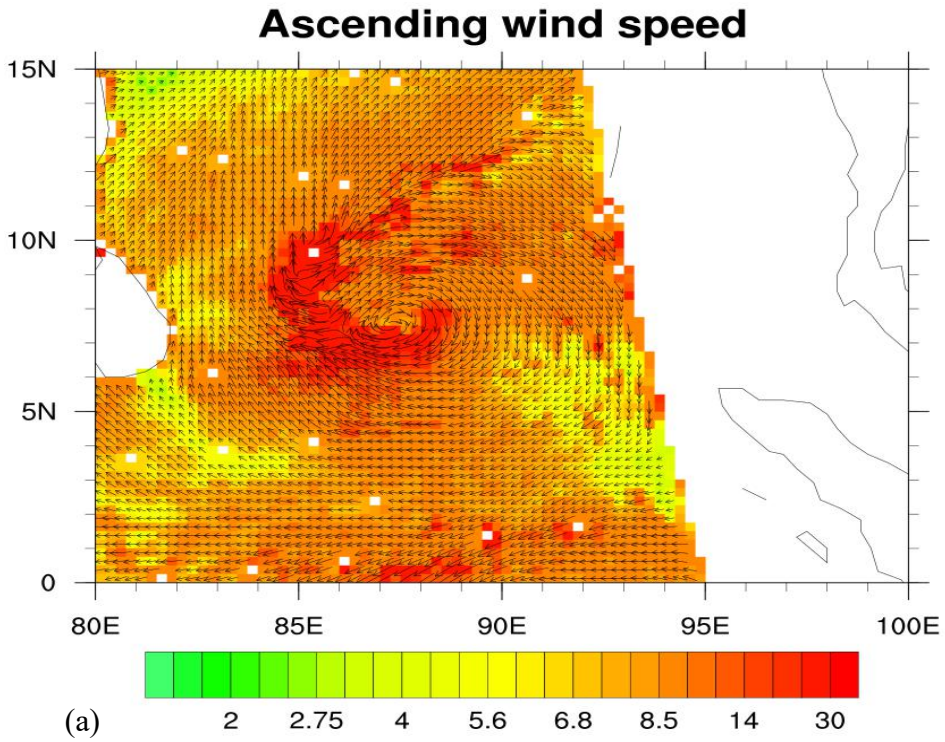

(a)

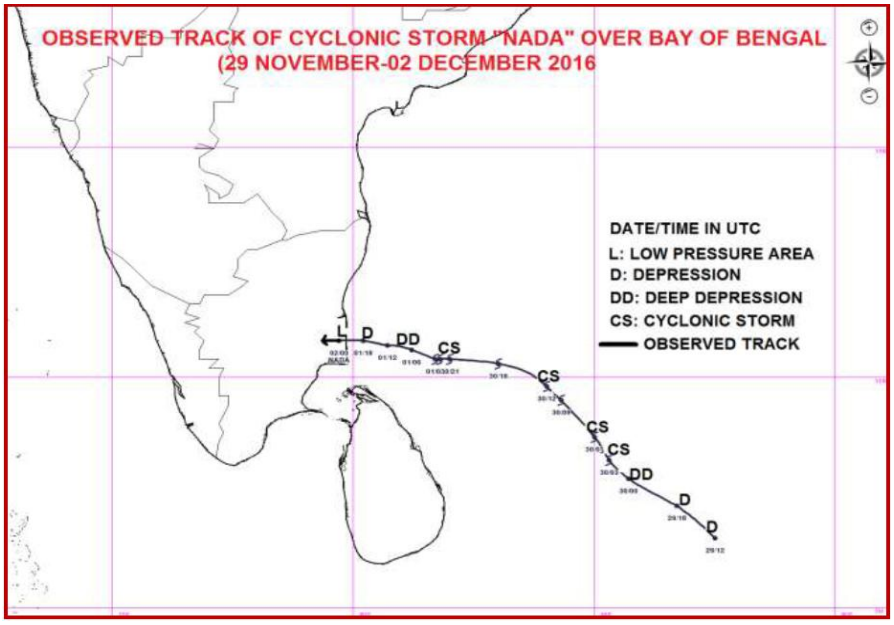

(b)

Fig. 5 The cyclone NADA (a) at its mature stage as observed from SCATSAT-1 and (b) the track of NADA as observed by IMD

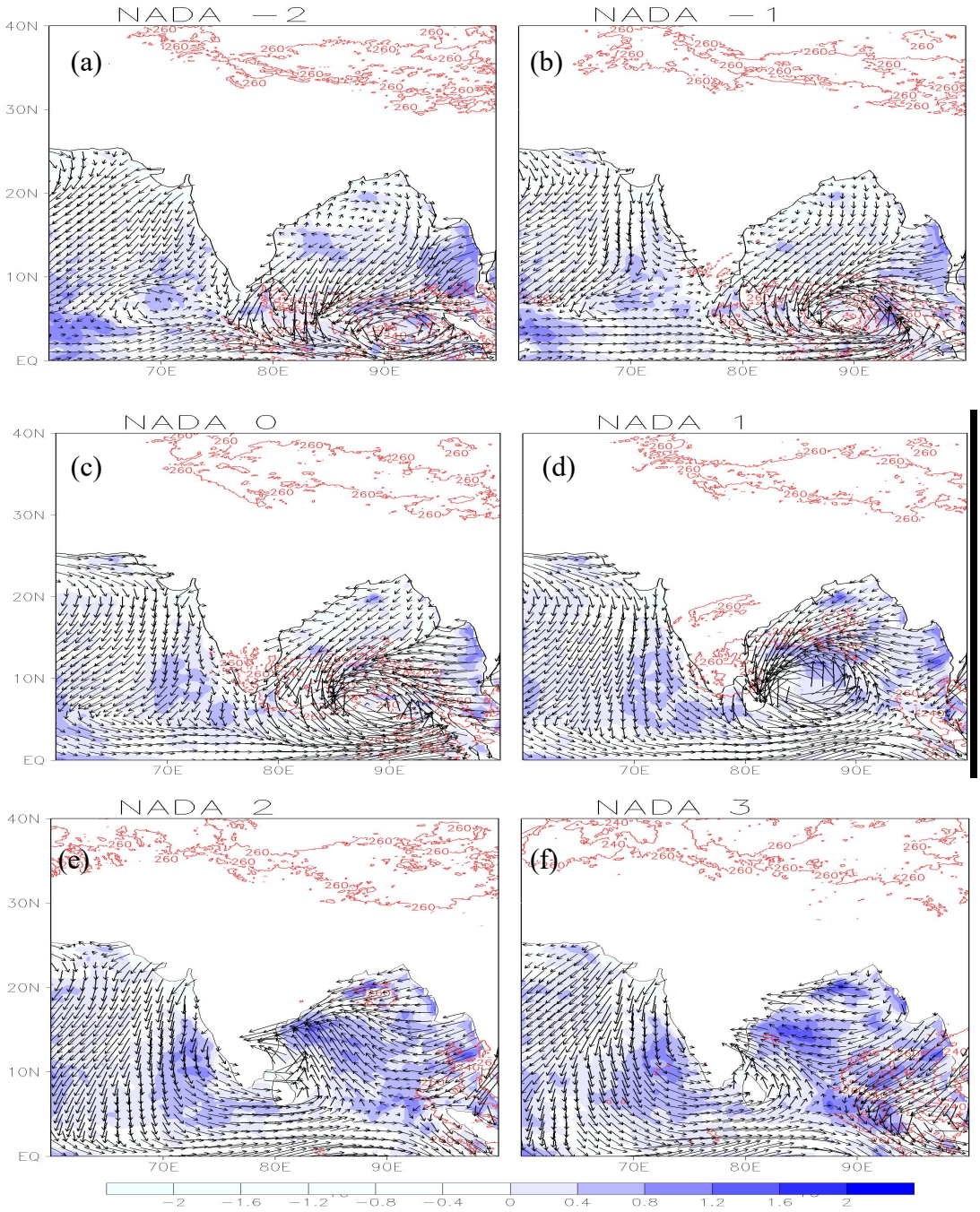

Fig. 6 Analysis of SST anomaly (shaded) and ocean vector wind at 10m (vector) along with position of cloud cluster as obtained from brightness temperature (red contour) for (a) 2 days before (b) 1 day before NADA along with (c) day 1 (d) day 2 (e) day 3 and (f) day 4 of NADA

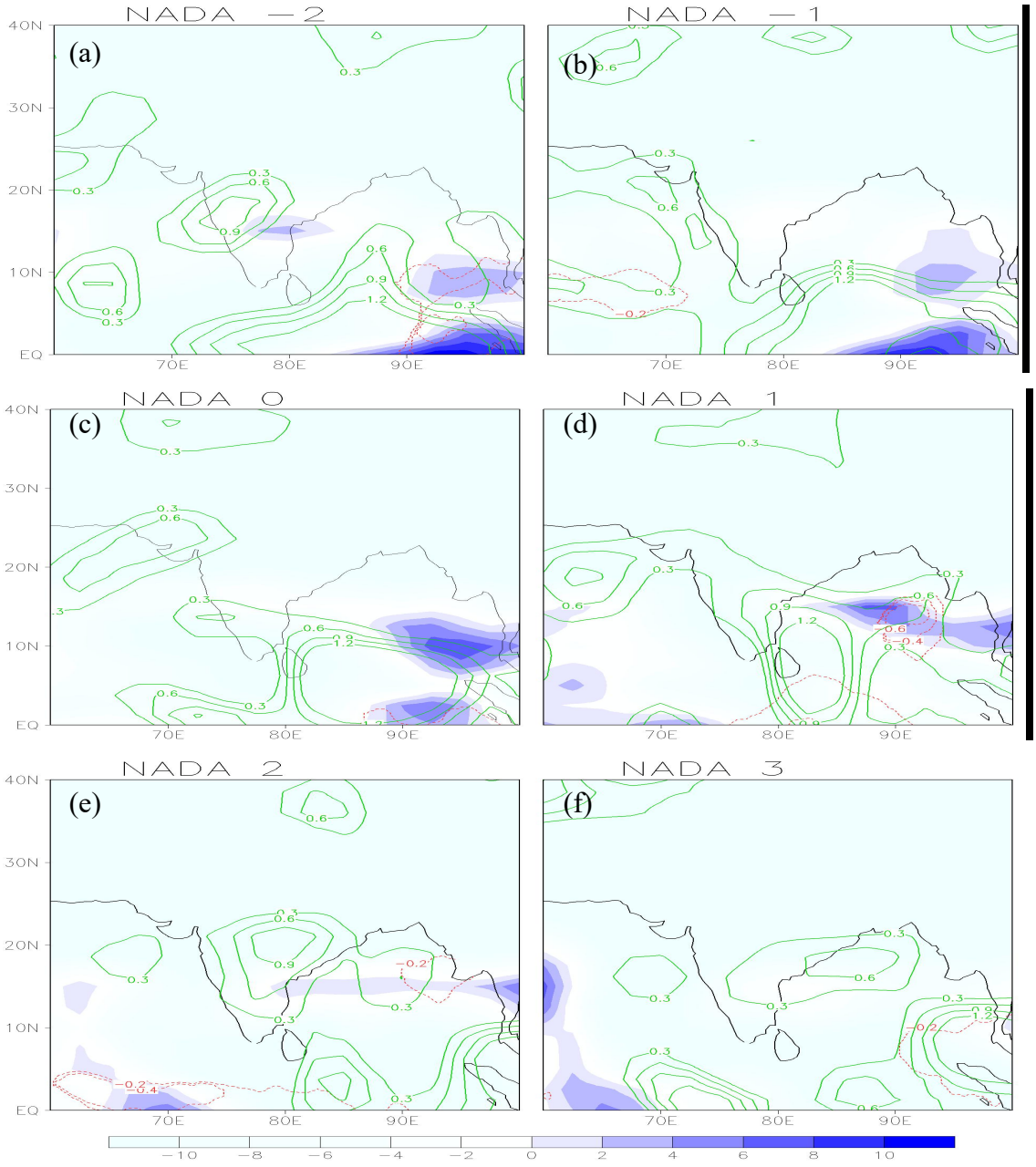

Fig. 7 Diagram shows wind shear between 850 hPa and 200 hPa (shaded), low level convergence (negative red contour) and upper level (200 hPa) divergence (positive green contour) for (a) 2 days before (b) 1 day before NADA along with (c) day 1 (d) day 2 (e) day 3 and (f) day 4 of NADA

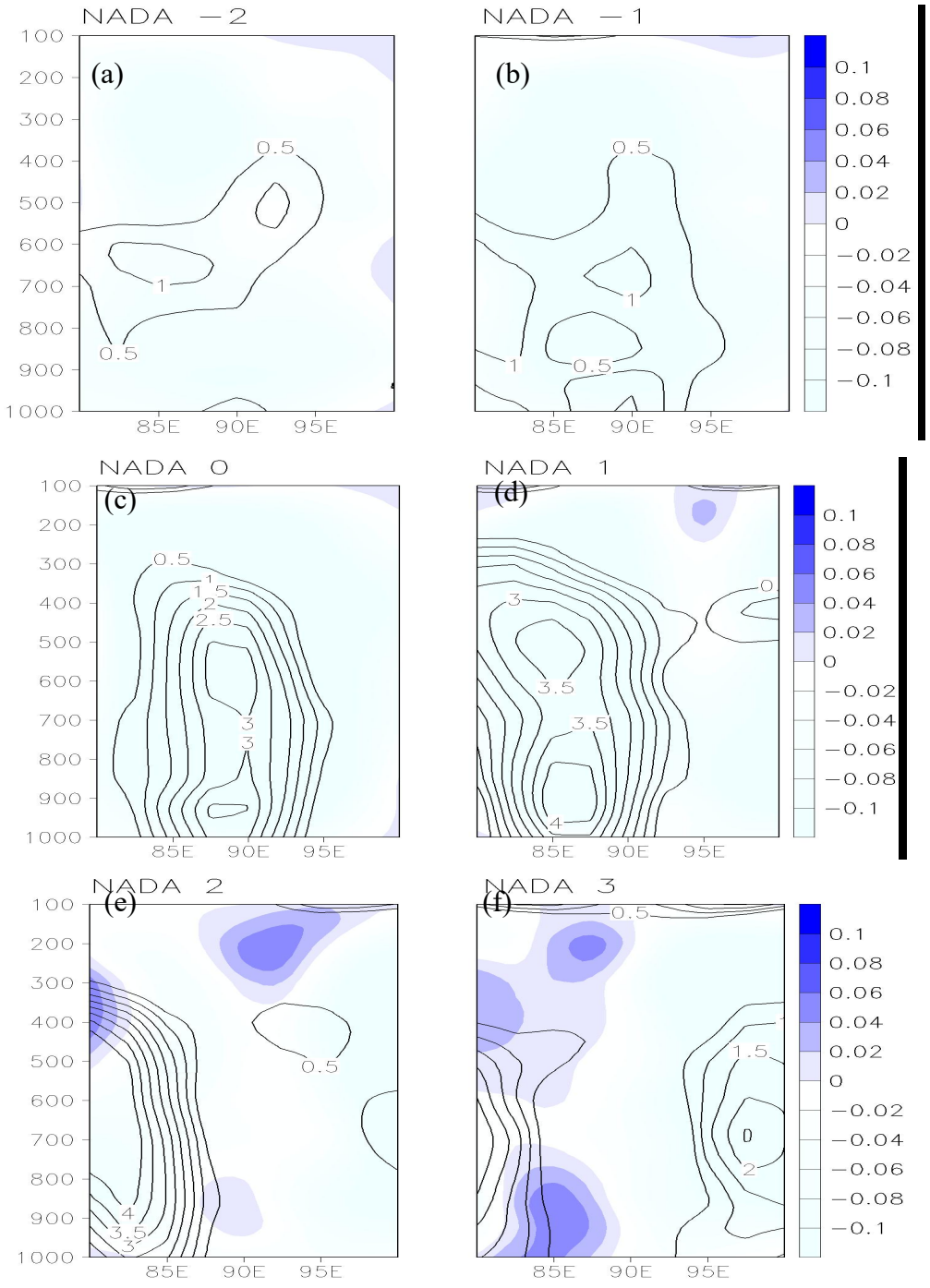

Fig. 8 Diagram shows vertical profile of positive vorticity (contour) and vertical velocity (shaded) for (a) 2 days before (b) 1 day before NADA along with (c) day 1 (d) day 2 (e) day 3 and (f) day 4 of NADA

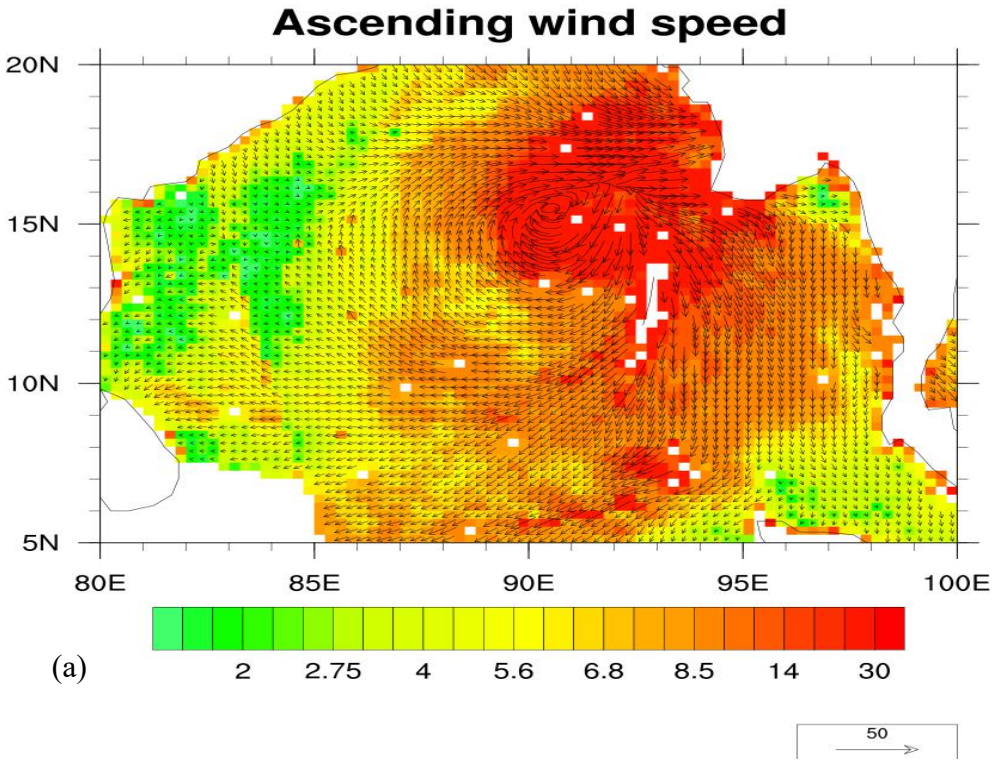

(a)

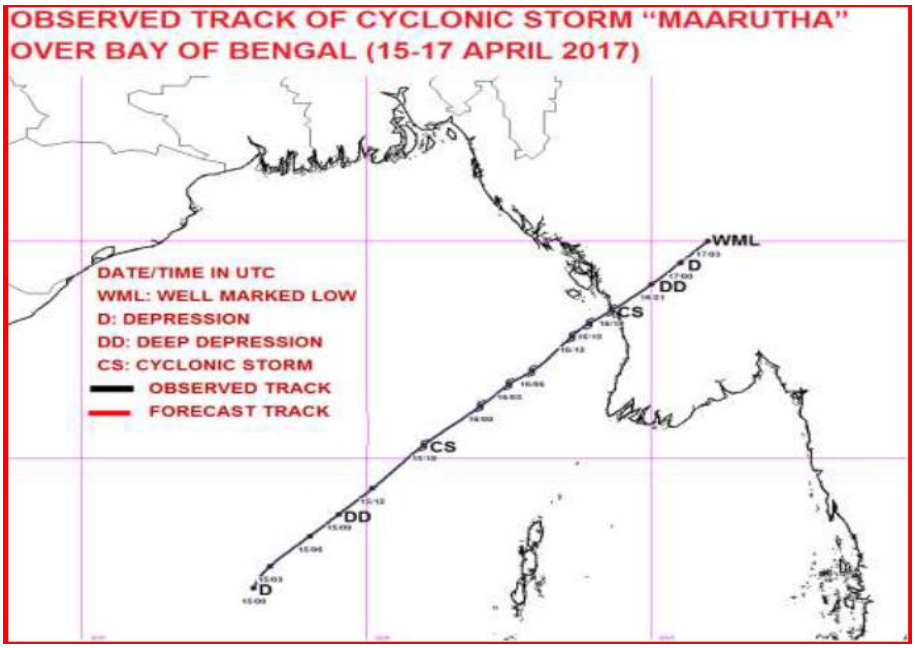

(b)

Fig. 9 The cyclone MAARUTHA (a) at its mature stage as observed from SCATSAT-1 and (b) the track of MAARUTHA as observed by IMD

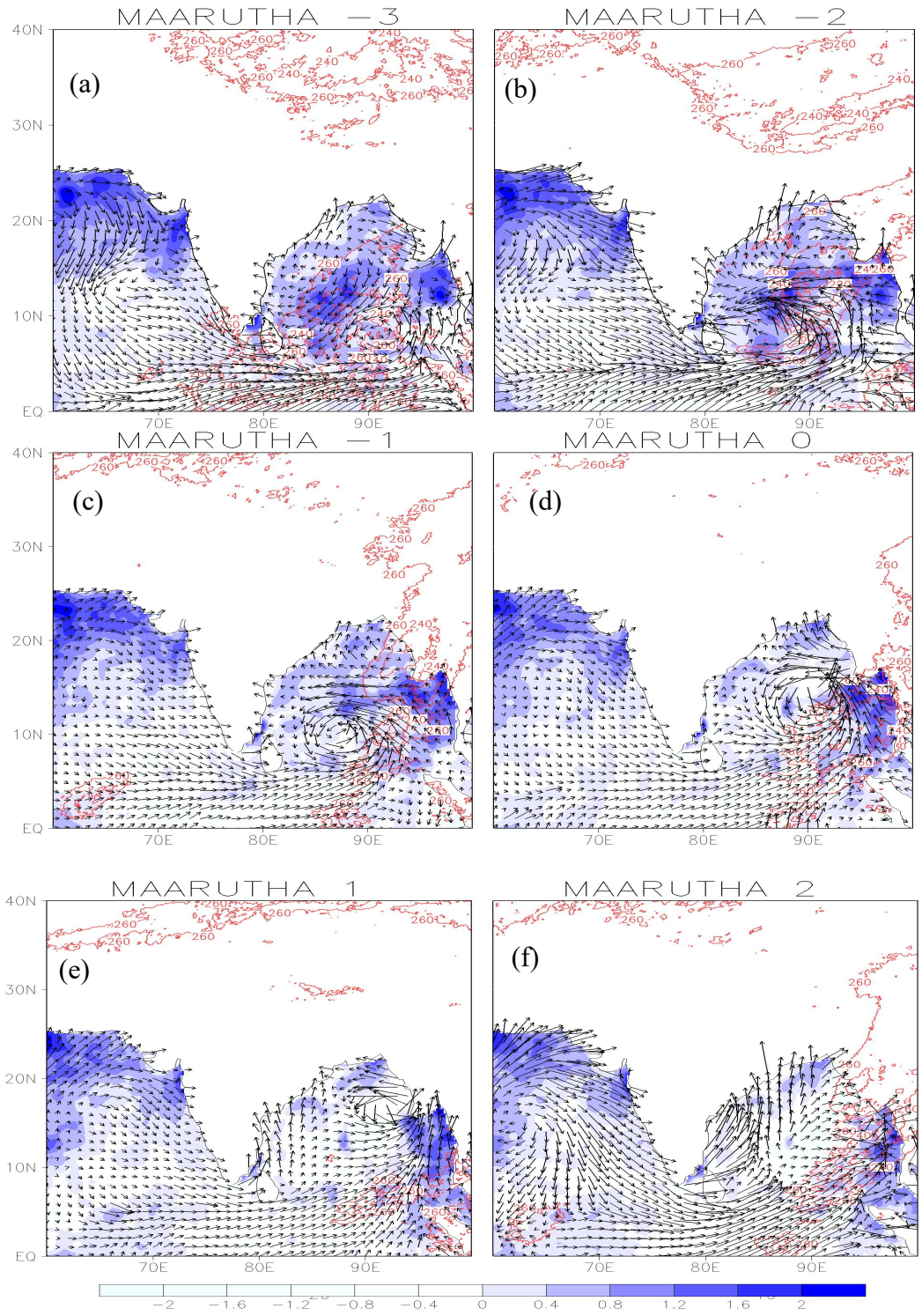

Fig. 10 Analysis of SST anomaly (shaded) and ocean vector wind at 10m (vector) along with position of cloud cluster as obtained from brightness temperature (red contour) for (a) 3 days before (b) 2 day before (c) 1 day before MAARUTHA along with (d) day 1 (e) day 2 and (f) day 3 of MAARUTHA

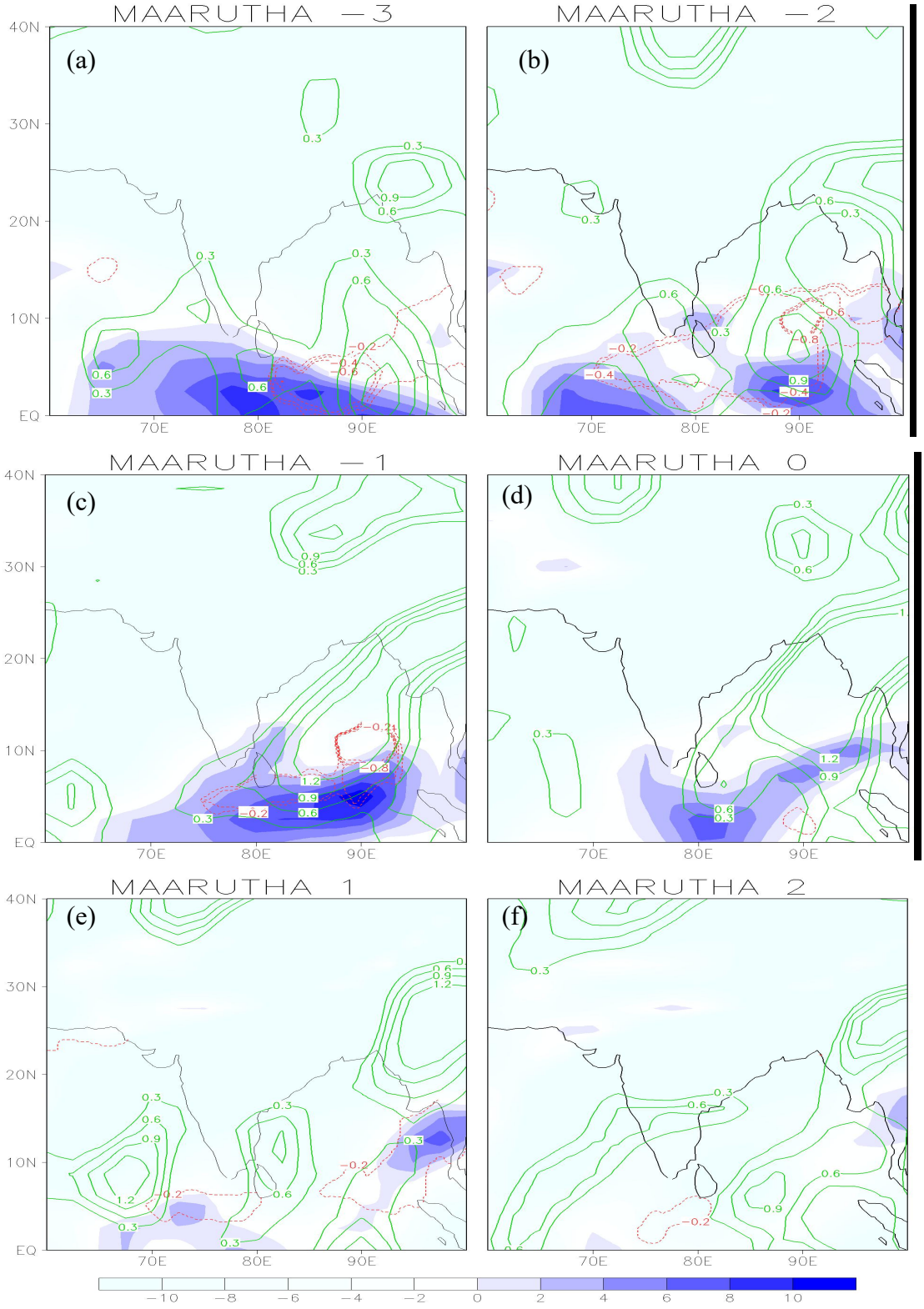

Fig. 11 Diagram shows wind shear between 850 hPa and 200 hPa (shaded), low level convergence (negative red contour) and upper level (200 hPa) divergence (positive green contour) for (a) 3 days before (b) 2 day before (c) 1 day before MAARUTHA along with (d) day 1 (e) day 2 and (f) day 3 of MAARUTHA

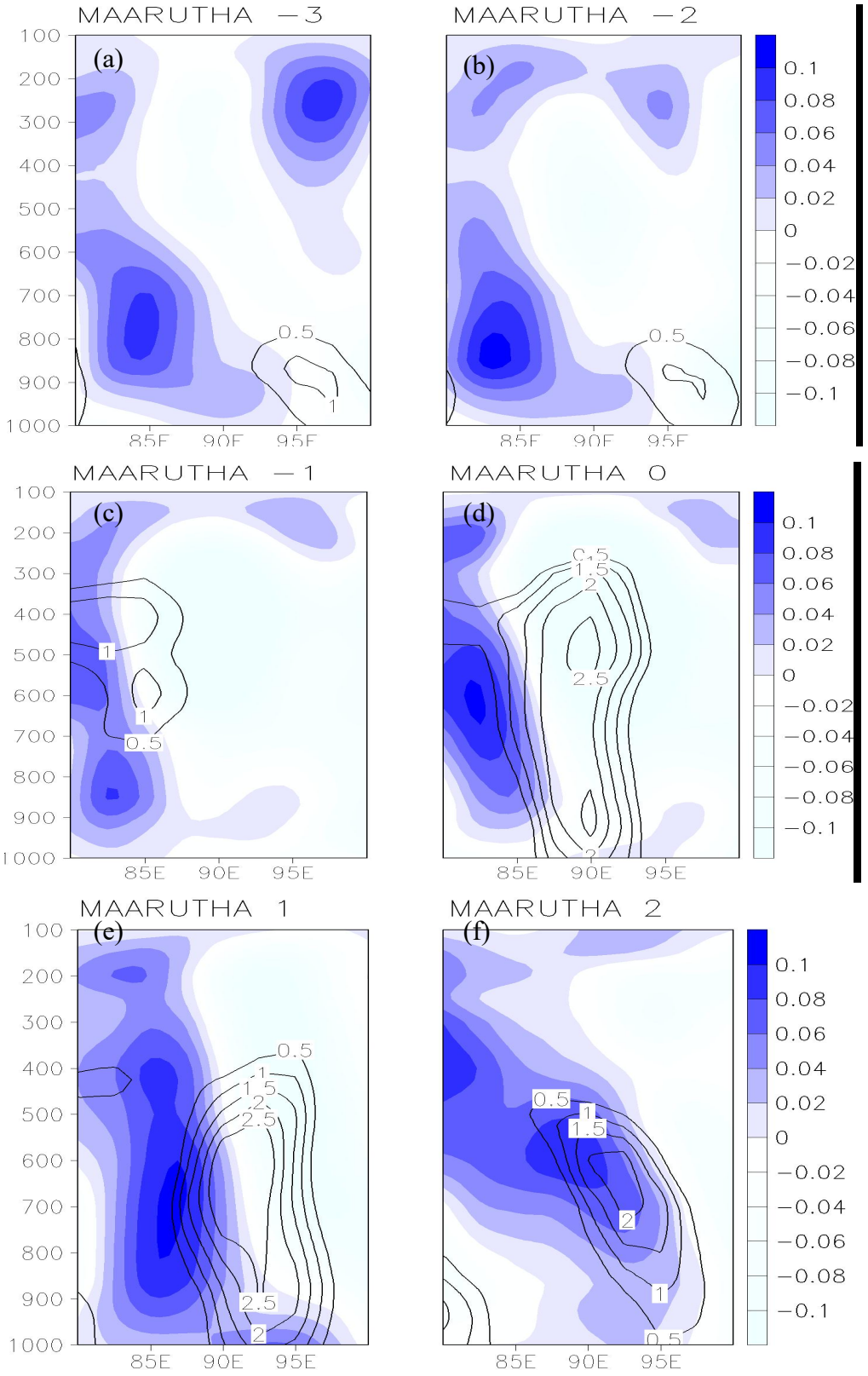

Fig. 12 Diagram shows vertical profile of positive vorticity (contour) and vertical velocity (shaded) for (a) 3 days before (b) 2 day before (c) 1 day before MAARUTHA along with (d) day 1 (e) day 2 and (f) day 3 of MAARUTHA

References

[1] Aberson SD (2001) The Ensemble of tropical cyclone track forecasting models in the North Atlantic basin (1976–2000). Bull Am Meteorol Soc 82:1895–1904

[2] BhaskarRao DV, HariPrasad D (2006) Numerical prediction of the Orissa super cyclone (1999): Sensitivity to the parameterisation of convection, boundary layer and explicit moisture processes. Mausam 57(1):61–78

[3] Chaudhuri S, Dutta D, Goswami S, Middey A (2014) Track and intensity forecast of tropical cyclones over the North Indian Ocean with multilayer feed forward neural nets. Meteorol Appl 22:563 – 575

[4] Deshpande M, Pattnaik S, Salvekar PS (2010) Impact of physical parameterization schemes on numerical simulation of super cyclone Gonu. Nat Hazards 55(2):211-231

[5] Emanuel K (2003) Tropical cyclones. Annu Rev Earth Pl Sc 31:75-104

[6] Franklin JL, McAdie CJ, Lawrence MB (2003) Trends in Track forecasting for Tropical Cyclones threatening the United States, 1970–2001. Bull Am Meteorol Soc 84:1197-1203

[7] George JE, Gray WM (1976) Tropical cyclone motion and surrounding parameter relationships. J Appl Meteorol 15:1252–1264. https://doi.org/10.1175/1520-0450(1976)015<1252:TCMASP>2.0.CO;2

[8] Holland GJ (1983) Tropical Cyclone Motion: Environmental interaction plus a Beta Effect. J Atmos Sci 40:328–342

[9] Jaiswal N, Kumar P, Kishtawal C (2019) SCATSAT-1 wind products for tropical cyclone monitoring, prediction and surface wind structure analysis. Curr Sci 117(6):983-992

[10] Kalnay E, Kanamitsu M, Kistler R et al (1996) The NCEP/NCAR 40-year reanalysis project. Bull Am Meteorol Soc 77: 437–472

[11] Knapp KR, Ansari S, Bain CL, Bourassa MA, Dickinson MJ, Funk C, Helms CN, Hennon CC, Holmes CD, Huffman GJ, Kossin JP, Lee HT, Loew A, Magnusdottir G (2011) Globally gridded satellite observations for climate studies. Bull Am Meteorol Soc 92:893-907

[12] Leroux MD, Wood K, Elsberry RL, Cayanan EO, Hendricks E, Kucas M, Otto P, Rogers R, Sampson B, Yu Z (2018) Recent Advances in Research and Forecasting of Tropical Cyclone Track, Intensity, and Structure at Landfall. Tropical Cyclone Research and Review 7(2):85-105. https://doi.org/10.6057/2018TCRR02.02

[13] Mohanty UC, Gupta A (2008) Deterministic methods for prediction of tropical cyclone tracks. In: Modelling and monitoring of coastal marine processes. Springer, Berlin, pp 141–170

[14] Mohanty UC, Nadimpalli R, Mohanty S, Osuri KK (2019) Recent advancements in prediction of tropical cyclone track over north Indian Ocean basin. Mausam 70(1):57-70

[15] Mohapatra M, Nayak DP, Sharma RP, Bandyopadhyay BK (2013) Evaluation of official tropical cyclone track forecast over north Indian Ocean issued by India Meteorological Department. J Earth Syst Sci 122(3):589–601

[16] Mohapatra M, Nayak DP, Sharma M, Sharma RP, Bandyopadhyay BK (2015) Evaluation of official tropical cyclone landfall forecast issued by India Meteorological Department. J Earth Syst Sci 124: 861–874. https://doi.org/10.1007/s12040-015-0581-x

[17] Osuri KK, Mohanty UC, Routray A, Makarand AK, Mohapatra M (2012) Sensitivity of physical parameterization schemes of WRF model for the simulation of Indian seas tropical cyclones. Nat Hazards 63:1337-1359

[18] Osuri KK, Mohanty UC, Routray A, Mohapatra M, Niyogi D (2013) Real-Time Track Prediction of Tropical Cyclones over the North Indian Ocean Using the ARW Model. J Appl Meteor Climatol 52:2476–2492. https://doi.org/10.1175/JAMC-D-12-0313.1

[19] Rama Rao YV, Nagaratna K, Joardar D, Sharma A, Kumar A (2015) Evaluation of short range forecast for tropical cyclones over North Indian Ocean using TIGGE data. Mausam 66:349–356

[20] Rappaport EN, Franklin JL, Avila LA et al (2009) Advances and challenges at the National Hurricane Center. Wea Forecasting 24:395–419. https://doi.org/10.1175/2008WAF2222128.1

[21] Reynolds RW, Smith TM, Liu C, Chelton DB, Casey KS, Schlax MG (2007) Daily high-resolution-blended analyses for sea surface temperature. J Climate 20:5473–5496

[22] Srinivas CV, Yesubabu V, Hari Prasad, KBRR, Venkatraman B, Ramakrishna SSVS (2012) Numerical simulation of cyclonic storms FANOOS, NARGIS with assimilation of conventional and satellite observations using 3-DVAR. Nat Hazards 63(2): 867-889